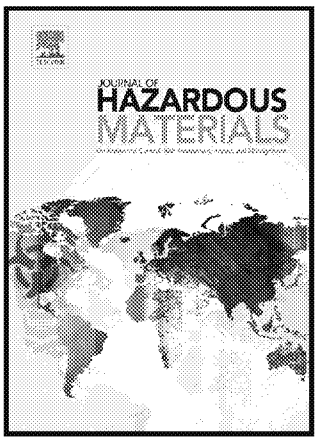


# Chronic exposure to PFO4DA and PFO5DoDA, two perfluoroalkyl ether carboxylic acids (PFECAs), suppresses hepatic stress signals and disturbs glucose and lipid metabolism in male mice

Jiamiao Chen, Hongyuan Li, Jingzhi Yao, Hua Guo, Hongxia Zhang, Yong Guo, Nan Sheng, Jianshe Wang, Jiayin Dai

PII: S0304-3894(20)32954-X

DOI: https://doi.org/10.1016/j.jhazmat.2020.124963

Reference: HAZMAT124963

To appear in: *Journal of Hazardous Materials*

Received date: 24 August 2020
Revised date: 21 December 2020
Accepted date: 23 December 2020

Please cite this article as: Jiamiao Chen, Hongyuan Li, Jingzhi Yao, Hua Guo, Hongxia Zhang, Yong Guo, Nan Sheng, Jianshe Wang and Jiayin Dai, Chronic exposure to PFO4DA and PFO5DoDA, two perfluoroalkyl ether carboxylic acids (PFECAs), suppresses hepatic stress signals and disturbs glucose and lipid metabolism in male mice, *Journal of Hazardous Materials*, (2020) doi:https://doi.org/10.1016/j.jhazmat.2020.124963

# Chronic exposure to PFO4DA and PFO5DoDA, two perfluoroalkyl ether carboxylic acids (PFECAs), suppresses hepatic stress signals and disturbs glucose and lipid metabolism in male mice

Jiamiao Chen [a, b, 1], Hongyuan Li [b, 1], Jingzhi Yao [b], Hua Guo [b], Hongxia Zhang [b], Yong Guo [c], Nan Sheng [b], Jianshe Wang [b, d *], Jiayin Dai [b]

[a] Hebei University, Baoding 071002, Hebei Province, P.R. China.

[b] Key Laboratory of Animal Ecology and Conservation Biology, Institute of Zoology, Chinese Academy of Sciences, Beijing 100101, P.R. China.

[c] Key Laboratory of Organofluorine Chemistry, Shanghai Institute of Organic Chemistry, Chinese Academy of Sciences, Shanghai 200032, P.R. China.

[d] School of Pharmacy, Collaborative Innovation Center of Advanced Drug Delivery System and Biotech Drugs in Universities of Shandong, Key Laboratory of Molecular Pharmacology and Drug Evaluation (Yantai University), Ministry of Education, Yantai University, Yantai, Shandong Province, P.R. China.

* Corresponding to: Jianshe Wang, E-mail address: jianshewang@ioz.ac.cn, wangjs@ytu.edu.cn.

[1] These authors contributed to this work equally.



**Abstract**

Perfluoroalkyl ether carboxylic acids (PFECAs), including PFO4DA and PFO5DoDA, have been found in both surface water and volunteer blood samples from polluted regions. However, little knowledge is available on their potential bioaccumulation and health risk. In the present study, the half-lives of PFO4DA and PFO5DoDA in male mouse serum were 24 h and nearly 43 d, respectively, indicating markedly increased difficulty in eliminating PFO5DoDA from the body. After 140 d daily exposure both PFO4DA and PFO5DoDA (10 μg/kg/d) increased body weight.

Hepatomegaly was the most sensitive phenomenon after exposure treatment, with occurrence even in the 2 μg/kg/d exposure groups. RNA-seq analysis supported a similar but stronger effect of PFO5DoDA compared with PFO4DA. A wide array of genes involved in stimulus sensing and response were suppressed. In addition to weight gain, hyperglycemia was also observed after treatment. Increased glucose and decreased pyruvate and lactate levels in the liver supported a reduction in glycolysis, consistent with the reduction in the key regulator *Pfkfb3*. In conclusion, chronic PFO4DA and PFO5DoDA exposure suppressed stress signals and disturbed glucose and lipid metabolism in the liver. The longer serum half-life and stronger hepatic bioaccumulation of PFO5DoDA, at least partially, contributed to its stronger hepatotoxicity than that of PFO4DA.

**Keywords**: PFO4DA, PFO5DoDA, bioaccumulation, stress sensor, hepatotoxicity

## 1. Introduction

Per- and polyfluoroalkyl substances (PFASs) are a class of human-made organic chemicals characterized by stable carbon-fluorine bonds. These bonds endow PFASs with unique physicochemical properties, such as water and oil repellence, high temperature resistance, and reduced surface tension, resulting in their substantial production and diverse application in industrial and day-to-day products (Buck, *et al.*, 2011). Two of the most widespread PFASs are perfluorooctane sulfonate (PFOS) and perfluorooctanoic acid (PFOA), which have been frequently detected in drinking water and other environmental matrices (Mak, *et al.*, 2009). With their widespread global occurrence and increased concern regarding their potential hazards, the

production and usage of PFOS and PFOA were banned or severely restricted (ECHA, 2019; Secretariat, 2019). Following the introduction of these new regulations, fluoropolymer producers and manufacturers sought novel fluorinated alternatives (Wang, *et al.*, 2013; Wang, *et al.*, 2018; Xiao, 2017), including perfluoroalkyl ether carboxylic acids (PFECAs) such as hexafluoropropylene oxide dimer acid (HFPO-DA) ammonium salt (GenX) from DuPont and 4,8-dioxa-3H-perfluorononanoate ammonium salt (ADONA) from 3M/Dyneon (Wang, *et al.*, 2013; Xiao, 2017). GenX have been reported at relatively high levels in surface water and drinking water (Gebbink, *et al.*, 2017), and ADONA was detected in part of local resident plasma samples (Fromme, *et al.*, 2017). Their potential impact on environmental health has also been investigated (Blake, *et al.*, 2020; Conley, *et al.*, 2019; Gordon, 2011). Recently, other PFECAs with the $F_3C–(OCF_2)_n–CO_2$ (n = 2–5) structure, including perfluoro-(3,5,7,9-tetraoxadecanoic) acid (PFO4DA) and perfluoro-3,5,7,9,11-pentaoxadodecanoic acid (PFO5DoDA), have been discovered in both environmental samples and finished drinking water downstream of a fluoropolymer manufacturing facility in the Cape Fear River, North Carolina (Hopkins, *et al.*, 2018; Strynar, *et al.*, 2015; Sun, *et al.*, 2016; Zhang, *et al.*, 2019). These PFECAs are believed to be byproducts from fluoromonomer and Nafion membrane production (Zhang, *et al.*, 2019). Both PFO4DA and PFO5DoDA have been detected in 99% and 88% of blood samples from volunteers in Wilmington, with median blood concentrations of >2.0 ng/mL and <0.5 ng/mL, respectively (Kotlarz, *et al.*, 2020). These two chemicals have also been detected in surface water in the Xiaoqing River in China (data unpublished), as well as in blood samples of near-by residents

(frequent detection > 95%, and the median concentration of PFO4DA and PFO5DoDA was 0.14 and 0.99 ng/mL, respectively) (Yao, *et al.*, 2020).

Although studies have reported on the occurrence of PFO4DA and PFO5DoDA in surface water and human serum samples, few studies have addressed their bioaccumulation or health risk potential (Guo, *et al.*, 2019; Sun, *et al.*, 2019; Wang, *et al.*, 2020). Using KOWWIN (v1.68) from the USEPA EPI (Estimation Programs Interface) Suite, the estimated log octanol-water partition coefficients (log*Kow*) of PFO4DA and PFO5DoDA are 5.25 and 7.17, respectively, higher than the estimated log*Kow* (4.81) for PFOA. However, Guo et al. reported a relatively weaker accumulation potential of PFO4DA compared with that of PFOA in mice (Guo, *et al.*, 2019). For surfactants, log*Kow* is not actually a valid descriptor for bioaccumulation potential assessment. Furthermore, partitioning properties is not reliable as screening criteria for the bioaccumulation ability of chemicals, as many factors, including protein-binding properties and renal clearance, can determine bioaccumulation ability (Tonnelier, *et al.*, 2012). Few studies have addressed the biological effects of PFO4DA and PFO5DoDA (Guo, *et al.*, 2019; Sun, *et al.*, 2019; Wang, *et al.*, 2020). For example, mice treated with 2 and 10 mg/kg/d of PFO4DA for 28 days are reported to display a marked increase in relative liver weight, although lower doses (0.4 mg/kg/d) appear to have no observable effect (Guo, *et al.*, 2019). To the best of our knowledge, however, no data are currently available regarding the biological effects of PFO5DoDA on mice. Given that PFO4DA and PFO5DoDA have been detected in water and human blood samples in polluted regions, such as near the Cape Fear River in USA (Hogue, 2019; Hopkins, *et al.*, 2018; Strynar, *et al.*, 2015;

Sun, *et al.*, 2016; Zhang, *et al.*, 2019) and the Xiaoqing River in China, it is important that their characteristics in the human body as well as their potential health effects under long-term exposure are examined. In the current study, we explored (1) the potential bioaccumulation and elimination ability of PFO4DA and PFO5DoDA and (2) their chronic effects on the liver after prolonged treatment (140 d) in male mice.

## 2. Material and methods

### 2.1 Animals and treatments

PFO4DA ($C_6HF_{11}O_6K$, MW 417.2, > 98.0% purity) and PFO5DoDA ($C_7HF_{13}O_7K$, MW 483.16, > 98.0% purity) were synthesized by Dr. Yong Guo from the Shanghai Institute of Organic Chemistry, Chinese Academy of Sciences (CAS), China. Their chemical structures are shown in **Supplementary Fig. S1**. Specific pathogen-free (SPF)-grade male BALB/c mice (6–8 weeks old) were commercially provided by the Beijing Vital River Laboratory Animal Technology Company (China). Animals were housed at 25 °C and 60% relative humidity under a 12:12 h dark:light cycle. Food and drinking water were provided *ad libitum*. After one week of adaptation, the mice were used for toxicokinetic study following a single intravenous injection of 10 μg/kg body weight of PFO4DA or PFO5DoDA via the caudal vein. Blood samples were then repeatedly collected through retro-orbital bleeding for PFO4DA and PFO5DoDA detection during the following 7 days and 9 months, respectively. Another batch of mice were randomly divided into five groups (n = 12 per group), and treated with water or with 2 or 10 μg/kg/d of PFO4DA or

PFO5DoDA, respectively, by gavage for 140 d. At the end of exposure, the animals were fasted overnight and then sacrificed by cervical dislocation the next morning. Liver, spleen, kidneys, testes, and thymus were quickly removed, weighed, and snap frozen with liquid nitrogen before storage at –80 °C. Blood was also collected for biochemical indices and PFO4DA and PFO5DoDA analysis. All experimental procedures were approved by the Ethics Committee of the Institute of Zoology, CAS.

2.2 PFAS content detection in serum and liver

Extraction and detection of PFO4DA and PFO5DoDA in serum and liver samples were performed following our previous description (Wang, *et al.*, 2020). In brief, liver was homogenized with ultrapure water (1:10 w/v) with a sonicator. Serum and tissue homogenates (20 μL) were spiked with mass-labeled standard (0.5 ng), tetra-n-butylammonium hydrogen sulfate solution (0.5 M, 1 mL), $NaHCO_3/Na_2CO_3$ buffer (pH = 10, 2 mL), and methyl tert-butyl ether (MTBE) (4 mL). The supernatant organic phase was collected after vigorous shaking and centrifugation, then evaporated with nitrogen, and reconstituted in 200 μL of methanol. PFO4DA and PFO5DoDA were analyzed using ultra-performance liquid chromatography-tandem mass spectrometry (Exion LC-Triple Quad 5500, AB SCIEX, Framingham, MA, USA) under multiple reaction-monitoring (MRM) in negative electrospray ionization (ESI-) mode. A signal-to-noise ratio greater than 10 was defined as the limit of quantitation (LOQ). For quality assurance, method blanks and matrix spiked samples were also tested in each batch.

2.3 Toxicokinetic analysis

After a single intravenous injection, the serum elimination rate constants ($K_e$) of PFO4DA and PFO5DoDA were calculated in mice by fitting a single compartment model with first-order elimination. The serum elimination half-lives ($t_{1/2}$) of the two compounds were calculated by $t_{1/2} = \ln 2/K_e$.

2.4 Biochemical assay and hepatic histopathology

After 140 d daily exposure, the levels of glucose, pyruvate, and lactate in liver samples were detected using commercial kits from the Nanjing Jiancheng Bioengineering Institute, China. The levels of triglycerides and cholesterol in the liver were detected using kits from Applygen, China. The levels of glucose, alanine transaminase (ALT), aspartate aminotransferase (AST), cholesterol, triglycerides, and non-esterified free fatty acids (NEFF) in serum were measured using a Hitachi 7170A automatic analyzer (Japan). Liver samples were sliced and HE stained for histopathological observation.

2.5 RNA extraction

Total RNA was extracted from the liver samples after 140 d of exposure to PFO4DA and PFO5DoDA using TRIzol reagent (Thermo Fisher Scientific, USA). Total RNA quality was confirmed by 1% agarose gel electrophoresis and absorbance at 260 nm and 280 nm using a Nanodrop 2000 (Thermo Fisher Scientific, USA).

2.6 cDNA library construction and Illumina sequencing

After 140 d of treatment, the control and 10 μg/kg/d of PFO4DA and PFO5DoDA groups were selected for RNA-seq analysis by Annoroad Gene Technology Co. Ltd. (Beijing, China), as described in previous studies(Sheng, *et al.*, 2018; Wang J., *et al.*, 2017). The RNA (1 μg) from two individual mice in one group were pooled as one sample, and six animals in each group were used. In brief, mRNA was enriched with magnetic beads containing Oligo (dT) and disrupted into short fragments to synthesize single-stranded then double-stranded cDNA. After purification, sequencing adapter ligation, and fragment size selection, the sequencing library underwent polymerase chain reaction (PCR) amplification. The constructed library was sequenced using the Illumina HiSeq 2500 platform.

2.7 Sequence assembly, differentially expressed gene (DEG) identification, and KEGG enrichment analysis

After removing low-quality reads and adapter sequences, the clean reads were assembled and mapped to the reference genome via TopHat2. Gene expression was quantified using the reads per kilobase of exon model per million mapped reads (RPKM) method. Genes were considered differentially expressed with a fold-change $\geq 2$ and false positive rate (FDR) $< 0.05$ compared to the control. Pathway enrichment of DEGs was analysed using the Kyoto Encyclopedia of Genes and Genomes (KEGG) database, with corrected $p < 0.05$ considered significant.

2.8 Quantitative real-time PCR (qRT-PCR) and western blotting analysis

Both qRT-PCR and western blot analyses were performed as described previously (Sheng, *et al.*, 2018; Wang J. S., *et al.*, 2017) using liver total RNA and tissue homogenates after chronic exposure, with 18S rRNA and GAPDH used as the internal controls, respectively. Primer information for qRT-PCR is listed in **Supplementary Table S1**. The PFKPB3 (ab181861) and FGF21 (ab171941) antibodies were purchased from Abcam, USA, and the GAPDH antibody (60004-1-Ig) was purchased from Proteintech, USA.

2.9 Statistical analyses

Data were analysed using SPSS 18.0 software (SPSS Inc., Chicago, IL, USA) and presented as means ± SE. Differences between groups were determined using one-way analysis of variance (ANOVA) followed by Duncan's multiple range test. Here, $p < 0.05$ between groups was considered statistically significant.

**3. Results**

3.1 Toxicokinetic analysis of PFO4DA and PFO5DoDA

Toxicokinetic parameters for PFO4DA and PFO5DoDA were obtained after an intravenous injection using a single compartment model with first-order elimination kinetics. The PFO4DA peak in serum appeared 30 min after the 10 μg/kg/d injection, then declined exponentially, and was thoroughly cleared in serum after 7 d (**Fig. 1A**). The serum concentration-time

(logarithmically transformed) curve showed good linear fit (Adj. $R^2 = 0.97$). The calculated serum half-life of PFO4DA in male mice was 24 h. However, after the single intravenous injection of 10 μg/kg/d of PFO5DoDA, no sharp peak was observed in the serum samples. Serum PFO5DoDA gradually decreased to 12–17 ng/mL after 6–7 weeks, with 2–3 ng/mL still detected in sera after nine months (**Fig. 1B**). After linear fit (Adj. $R^2 = 0.99$), the calculated serum half-life of PFO5DoDA in male mice was 43 d, indicating increased difficulty in the elimination of PFO5DoDA.

3.2 Body and organ weight and serum biochemistry

After 140 d, male mice exposed to PFO4DA and PFO5DoDA showed an increase in body weight gain (**Fig. 2A**). Specifically, body weight gain was 7.84 g and 8.17 g in the 10 μg/kg/d PFO4DA and PFO5DoDA exposure groups, respectively, which were significantly elevated compared with that of the control group (6.86 g). Organ indices (organ weight/body weight × 100%) were used to explore the potential effects of exposure on organs. Results showed that most organ indexes showed no change in the PFO4DA and PFO5DoDA exposure groups compared to that in the control group, except for the liver (**Fig. 2B**). The liver weight index increased by 4.6% and 7.25% in the 2 and 10 μg/kg/d PFO4DA groups, respectively, compared with that in the control group. After PFO5DoDA treatment, relative liver weight increased by 5.83% and 21.81% in the 2 and 10 μg/kg/d groups, respectively. In the 10 μg/kg/d groups, PFO5DoDA treatment resulted in greater hepatomegaly than that by PFO4DA. However, these was no obvious lesion in their histopathological sections (**Supplementary Fig. S2**), and the serum indicators of

hepatocellular damage, i.e., ALT and AST, showed no change (**Fig. 2C**), implying that exposure did not lead to significant damage or necrosis in hepatocytes. However, due to the liver enlargement, our further toxicological analyses focused on the liver as a major target of PFO4DA and PFO5DoDA.

3.3 PFO4DA and PFO5DoDA content in serum and liver after 140 d of exposure

After 140 d of exposure, serum PFO4DA concentrations in the 2 and 10 μg/kg/d treatment groups were 2.00 and 7.78 ng/mL, respectively (**Fig. 3A**). For PFO5DoDA, serum concentrations in the 2 and 10 μg/kg/d treatment groups were 37.65 and 140.82 ng/mL, respectively, which were markedly higher than that in the corresponding PFO4DA groups. In addition, much higher liver concentrations were found in the PFO5DoDA groups than in the corresponding PFO4DA groups (**Fig. 3B**). Specifically, liver concentrations of PFO4DA and PFO5DoDA were 9.48 and 54.49 ng/g and 1 725.57 and 5 790.73 ng/g in the 2 and 10 μg/kg/d treatment groups, respectively. These results indicated that the two compounds had greater liver concentrations than serum concentrations after 140 d of exposure. Here, concentrations of PFO4DA and PFO5DoDA were 7- and 41-fold higher, respectively, in liver than in serum in the 10 μg/kg/d treatment groups.

3.4 Illumina sequencing and hepatic gene alteration after chronic exposure

RNA-seq was carried out with liver samples from the control and 10 μg/kg/d PFO4DA/PFO5DoDA groups after 140 d of exposure. After removing low-quality reads and adapter sequences, the high-quality clean reads (**Supplementary Table S2**) were assembled into

transcripts and mapped to the reference genome (**Supplementary Table S3**). Transcriptome analysis showed chronic treatment changed the hepatic transcriptomic profile. In total, 221 (91 up-regulated; 130 down-regulated) and 707 (332 up-regulated; 375 down-regulated) genes were significantly changed in the 10 μg/kg/d PFO4DA and PFO5DoDA groups, respectively, compared to that in the control (**Fig. 4A**). Among them, 126 (45 up-regulated; 81 down-regulated) genes were shared in both exposure groups (**Supplementary Table S4**), accounting for 57.0% and 17.8% of total changed genes in PFO4DA and PFO5DoDA groups, respectively. These results implied a stronger effect of PFO5DoDA than PFO4DA on transcriptomic changes in the liver. KEGG enrichment analysis revealed three shared pathways by the PFO4DA and PFO5DoDA groups, i.e., mitogen-activated protein kinase (MAPK) signaling, which responds to cellular stress, and peroxisome proliferators-activated receptor (PPAR) and insulin resistance signaling, which are involved in glucose and lipid metabolism (**Fig. 4B**). Some shared DEGs, including but not limited to inhibin beta-B (*Inhbb*), interleukin 1 receptor, type I (*Il1r1*), tyrosine aminotransferase (*Tat*), Ras-association domain family 2 (*Rassf2*), and SMAD family member 6 (*Smad6*), were verified by qRT-PCR using liver samples from individuals different to those used for RNA-seq. Most showed a similar trend between the qRT-PCR and RNA-seq results (**Fig. 4C**).

3.5 Expression of stress sensors

Many genes involved in stress were suppressed after long-term exposure to 10 μg/kg/d of PFO4DA and PFO5DoDA (**Fig. 5A**), including growth arrest and DNA-damage-inducible 45 beta (*Gadd45b*), CCAAT enhancer binding protein (C/EBPs) family members, such as *C/EBP zeta*

(*Ddit3*, also known as *Chop*) and C/EBP delta (*Cebpd*), and heat shock protein family A (Hsp70) member 1A (*Hspa1a*), which maintains protein homeostasis during cellular stress. In addition to the above stress sensors and indicators, key members involved in the p53-axis, including tumor protein 53-induced nuclear protein 1 (*Tp53inp1*) and cyclin-dependent kinase inhibitor 1A (*Cdkn1a*, also known as *P21*), and a member of the activating protein-1 family, c-Jun dimerization protein (*Jdp2*), were also suppressed following PFO4DA and PFO5DoDA treatment. The reduced mRNA levels of the above genes were further confirmed using qRT-PCR (**Fig. 5B**). Results demonstrated the strong suppression of a wide range of transcriptional factors and functional genes involved in stimulus sensing after long-term exposure to PFO4DA and PFO5DoDA.

3.6 Glucose and lipids in liver

Exposure to 10 μg/kg/d of PFO4DA and PFO5DoDA for 140 d increased glucose levels in the mouse liver samples (**Fig. 6A**). Glucose levels increased from 0.21 mmol/g protein in the control group to 0.27 and 0.25 mmol/g protein in the 10 μg/kg/d PFO4DA and PFO5DoDA groups, respectively. As a glycolysis product, liver pyruvate concentrations in the 10 μg/kg/d PFO4DA and PFO5DoDA groups were 12.08 and 12.20 nmol/g protein, respectively, which were about 25% lower than that in the control group (16.04 nmol/g protein). Although no change in liver lactate level was observed in the 10 μg/kg/d PFO4DA group, it decreased by 12.75% in the 10 μg/kg/d PFO5DoDA group compared to that in the control group. Levels of total cholesterol and triglycerides in the liver were 169.9 and 540.6 μmol/g in the 10 μg/kg/d PFO5DoDA group, which were 26.5% and 15.6% lower than that in the control, respectively. In the 10 μg/kg/d

PFO4DA group, although total cholesterol exhibited no change compared with the control, triglycerides decreased by 15.6%. Serum glucose increased from 1.94 and 2.43 mmol/L in the control and 10 μg/kg/d PFO4DA groups, respectively, to 3.93 mmol/L in PFO5DoDA group (**Fig. 6B**). Serum cholesterol did not change after treatment. However, compared to that in the control group (2.04 mmol/L), serum triglycerides increased by 30% and 21% (to 2.65 and 2.46 mmol/L) in the 10 μg/kg/d PFO4DA and PFO5DoDA groups, respectively. Serum NEFF levels were 3.48 and 3.39 mmol/L in the PFO4DA and PFO5DoDA groups, respectively, indicating a 31% and 28% increase compared to that in the control group (2.66 mmol/L). The dramatic down-regulation of 6-phosphofructo-2-kinase/fructose-2,6-bisphosphatase 3 (*Pfkfb3*) and fibroblast growth factor 21 (*Fgf21*) in RNA-seq after exposure to 10 μg/kg/d of PFO4DA and PFO5DoDA was further verified by qRT-PCR and western blotting. (**Fig. 6C**).

## 4. Discussion

### 4.1 Bioaccumulation of PFO4DA and PFO5DoDA in liver contributed to their dominant hepatotoxicity

Many studies have reported on the occurrence of hepatomegaly in rodents after treatment with both legacy PFASs and their alternatives (Lau C., *et al.*, 2007; Sheng, *et al.*, 2018; Wang J. S., *et al.*, 2017). For example, Guo *et al.* found hepatomegaly accompanied by an increase in serum ASL and ALT levels in male mice following exposure to 2 and 10 mg/kg/d of PFO4DA via oral gavage for 28 d (Guo, *et al.*, 2019). In the present study, enlargement of the liver was also

observed after 140-d continuous exposure to both 2 and 10 μg/kg/d of PFO4DA and PFO5DoDA. However, unchanged histopathological results and serum levels of ASL and ALT indicated no obvious damage or necrosis in the liver, which may be due to the relatively low exposure doses in the present study. After 140 d of exposure, the serum level of PFO4DA in the 2 μg/kg/d group was 2 ng/mL, similar to that reported in the blood of residents from Wilmington (Hogue, 2019). These results indicate that hepatomegaly is a dominant and sensitive general phenomenon induced by PFO4DA and PFO5DoDA exposure in rodents. Although hepatomegaly has not been reported after PFAS exposure in non-rodents, other potential harmful effects need to be investigated.

Although PFO4DA and PFO5DoDA have a similar molecular structure, their elimination half-lives were markedly different. For example, half of PFO4DA was cleared from serum within 24 h, whereas PFO5DoDA required 43 d. A longer chain length tends to result in a longer $t_{1/2}$ time in legacy perfluorocarboxylic acids (PFACs), as observed in rats (Ohmori, *et al.*, 2003). Here, the increased $-OCF_2$ in PFO5DoDA compared with PFO4DA resulted in different toxicokinetic characteristics and a much slower elimination rate in mice. Studies have shown that legacy PFASs, such as PFOA, are predominantly distributed in the serum and liver after both single and repeated exposure in rodents (Dewitt, 2015). In the current study, after 140 d of exposure, concentrations of PFO4DA and PFO5DoDA were higher in the liver than serum. Specifically, 7- and 41-fold higher concentrations of PFO4DA and PFO5DoDA, respectively, were observed in the liver than in serum in the 10 μg/kg/d treatment groups. We speculate that the greater accumulation of PFO4DA and PFO5DoDA in the liver contributed to their dominant effects on this organ. In addition, the

slower elimination of PFO5DoDA led to its higher accumulation in the liver and blood, resulting in greater adverse effects on the liver than PFO4DA following long-term exposure.

The liver/serum ratios did not change much in the two exposure groups. The ratio was 4.8 and 7.0, respectively, in 2 and 10 μg/kg group of PFO4DA, and the ratio was 45.9 and 41.1 in 2 and 10 μg/kg group of PFO5DoDA, respectively. The result indicated that PFO5DoDA showed stronger bioaccumulation ability in liver than that in PFO4DA, which may be due to the difference in their binding with biomolecular and clearance ability by kidney. As for one chemical, the bioaccumulation ability in tissues also changes under various exposure doses and durations. For example, the liver/serum ratio was even low than 1 after high dose (10 mg/kg/d for 28 continuous day) exposure of PFO4DA, indicating that higher content of PFO4DA was accumulated in serum than liver (Guo, *et al.*, 2019), while in our present study, liver contained more PFO4DA than serum. The lower liver/serum ratio in the former may be because that the chemical has reached its maximum limitation of protein binding or clearance capacity in the body.

However, blood concentrations after prolonged PFO4DA and PFO5DoDA exposure cannot be simply estimated based on a single intravenous injection. For example, the predicted serum PFO4DA content would be 90–180 ng/mL after continuous exposure to 10 μg/kg/d of PFO4DA. Our study showed that after 140 d of PFO4DA treatment at 10 μg/kg/d, the serum level of PFO4DA (7.78 ng/mL) was considerably smaller than the predicted value based on the single intravenous injection, implying that enhancement in the clearance of PFO4DA may be induced by prolonged exposure.

4.2 PFO4DA and PFO5DoDA suppressed a wide array of stress sensing signals

Among the DEGs identified after 10 μg/kg/d PFO4DA (221 genes) and PFO5DoDA (707 genes) exposure, 57.0% and 17.8% were shared by both treatments. The high number of shared DEGs between PFO4DA and PFO5DoDA treatment indicate that these two chemicals exert similar biological effects, which may be due to their similar molecular structure. The greater effect of PFO5DoDA than PFO4DA was consistent with its higher bioaccumulation ability in the liver. Among the enriched pathways, PPAR were share by both PFO4DA and PFO5DoDA treatment. Activation of PPARα is one known common mechanism of hepatic effects for PFASs (Lau C, *et al.*, 2007; Vanden Heuvel, *et al.*, 2006), and its activation may be associated with hepatomegaly and the metabolic alterations after PFO4DA and PFO5DoDA treatment. Although under relatively high dose, some PFASs activated PPARα and led to great induction of its target genes (Lau C, *et al.*, 2007; Vanden Heuvel, *et al.*, 2006), their low-dose and long-term effect is not clear yet. In our present study, after 10 μg/kg/d PFO4DA and PFO5DoDA treatment for 140 days, the alteration in PPAR pathway was enriched by KEGG enrichment analysis in both of the treatment groups. However, some of the classic PPARα target genes, such as *Cyp4a10* and acyl-coA thioesterase 1 (*Acot1*) were not changed in both PFO4DA and PFO5DoDA treatment groups. In addition, relatively few PPAR target genes were shared in both PFO4DA and PFO5DoDA groups. In my opinion, the structure of PFASs varied greatly, which may lead to great variation in their binding affinity and activating ability on PPARα. Therefore, the activation ability on PPAR pathway

between different PFASs need a thorough comparison, using both *in vitro* cell or biochemical assay, and *in vivo* animal studies.

Although ADONA and other PFECAs do not display the potential to cause genetic mutations (Gordon, 2011; Hogue, 2019), our PFO4DA and PFO5DoDA study demonstrated suppression effects on multiple stress sensors involved in DNA damage and cellular growth regulation, such as *Gadd45b*, *Ddit3*, and *Cebpd*. *Gadd45b* is implicated as a stress sensor and target of transforming growth factor (TGF) beta (Dan and Liebermann, 2013). *Ddit3* (*C/EBP zeta*) and *Cebpd* (*C/EBP delta*) are members of the C/EBP family, a family of basic leucine zipper (bzip) domain-containing transcription factors. Under multiple cellular stresses, *C/EBPs* are involved in the regulation of cellular apoptosis, differentiation, and growth via dimerization and DNA binding with their bzip domains (Benezra, *et al.*, 1990). *Ddit3* is frequently used as an indicator of endoplasmic reticulum stress and *Cebpd* transcription is considered a pro-inflammatory factor during acute-phase response (Ramji and Foka, 2002). In addition to *C/EBPs*, the expression of *Jdp2*, a bzip transcription factor belonging to the activating protein-1 family, was also down-regulated in our study after PFO4DA and PFO5DoDA treatment. *Jdp2* is believed to mediate signals from environmental oxidative stress to inhibit cell cycle progression via the p53 pathway (Nakade, *et al.*, 2017). The p53 pathway plays a critical role in stress response and tumor suppression (Kaiser and Attardi, 2018). Two key genes involved in the p53 pathway, i.e., *Tp53inp1* and *Cdkn1a*, were also strongly suppressed by PFO4DA and PFO5DoDA. The marked decrease in *Cdkn1a* after PFO4DA and PFO5DoDA treatment suggests a release on cell cycle

transitions in G1/S and G2/M, which facilitated hepatocellular proliferation. *TP53inp1*, also known as stress-induced protein (*Sip*), is an antiproliferative and proapoptotic stress-response gene, and its expression is up-regulated with agents that can induce cell proliferation arrest and/or apoptosis (Tomasini, *et al.*, 2002). The effects of PFASs on the p53 pathway have been reported previously (Cui, *et al.*, 2019; Sheng, *et al.*, 2018; Sun, *et al.*, 2019; Zhang, *et al.*, 2018). Consistent with our study, suppression of *Cdkn1a* transcription in mouse livers has been observed after exposure to hexafluoropropylene oxide trimer acid (HFPO-TA) (Sheng, *et al.*, 2018). We also found that *Hspa1a*, a stress-inducible gene that displays versatile cytoprotective properties (Levada, *et al.*, 2018), was suppressed by PFO4DA and PFO5DoDA exposure. Taken together, a wide range of stress-sensing and response genes were suppressed in male mice after long-term PFO4DA and PFO5DoDA treatment, which might jeopardize the adaptation ability of these animals to a variety of environmental stimuli and challenges.

4.3 PFO4DA and PFO5DoDA disturbed hepatic glucose and lipid metabolism

Glycolysis is a metabolic biological process that converts glucose to pyruvate and lactate, with the conversion from fructose-6-phosphate to fructose-1,6-bisphosphate by 6-phosphofructo-1-kinase (PFK-1) considered to be a rate-limiting step (Weber, 1977). Intracellular F2,6P2 is a potent activator of PFK-1, and is mainly regulated by the PFKFB bifunctional (both kinase and phosphatase activity) enzyme family (Pilkis, *et al.*, 1995). Of all PFKFB isoenzymes, PFKFB3 possesses the highest kinase to phosphatase activity ratio and is the key enzyme for sustaining glycolytic rates (Sakakibara, *et al.*, 1997). Here, *Pfkfb3* mRNA was

down-regulated by both PFO4DA and PFO5DoDA treatment, with a reduction in PFKFB3 protein also observed in the PFO5DoDA group. The suppression on *Pfkfb3* may have contributed to the observed increase in glucose and decrease in pyruvate and lactate levels in the liver. In terms of lipid metabolism, both triglycerides and total cholesterol tended to decrease in the liver but increase in circulation after chronic treatment. Legacy PFASs are known to interfere with lipid metabolism, especially lipid accumulation in the liver, accompanied by body weight decrease after high-dose exposure *in vivo* (Dewitt, 2015). In the present study, however, chronic low-dose PFO4DA and PFO5DoDA treatment induced a moderate increase in body weight, serum NEFF, and hyperglycemia. Although the mode of action was not clear, one key gene involved in metabolic regulation, *Fgf21*, was significantly decreased in the liver after PFO4DA and PFO5DoDA treatment. *Fgf21* plays an important role in maintenance of metabolic homeostasis and has emerged as a potential therapeutic target for diabetes and obesity (Kharitonenkov, *et al.*, 2005; Ohta and Itoh, 2014). Disruption of the *Fgf21* signaling pathway could contribute to a moderate increase in body weight after treatment. The signaling pathways involving in glucose and lipid metabolism disturbance may interact with those in stress suppression under chronic PFO4DA and PFO5DoDA treatment (**Fig. 7**). It has been reported that both *Pfkfb3* and *Fgf21* play important roles in metabolic regulation in response to physiological stimuli. For example, oncogenic Ras signaling regulates glucose metabolism via *Pfkfb3* (Shi, *et al.*, 2017) and *Fgf21* serves as a key regulator of energy homeostasis under liver stress and injury (Luo and McKeehan, 2013).

In conclusion, chronic exposure to PFO4DA and PFO5DoDA induced body weight increase and liver enlargement in male mice. Various genes involved in stress and metabolic regulation were suppressed after PFO4DA and PFO5DoDA treatment. In terms of hepatomegaly and suppression of stress responses, stronger effects were observed in the PFO5DoDA groups compared to the PFO4DA groups. This was at least partly the result of the longer serum half-life and stronger bioaccumulation ability of PFO5DoDA than PFO4DA.

## Acknowledgments

This work was supported by the National Key R&D Program of China (2019YFC1605104) and National Natural Science Foundation of China (21777160 and 21906160).

## References

Benezra, R., Davis, R. L., Lockshon, D., Turner, D. L., Weintraub, H., 1990. The protein Id: a negative regulator of helix-loop-helix DNA binding proteins. *Cell, 61*, 49-59.

Blake, B. E., Cope, H. A., Hall, S. M., Keys, R. D., Mahler, B. W., McCord, J., Scott, B., Stapleton, H. M., Strynar, M. J., Elmore, S. A., Fenton, S. E., 2020. Evaluation of Maternal, Embryo, and Placental Effects in CD-1 Mice following Gestational Exposure to Perfluorooctanoic Acid (PFOA) or Hexafluoropropylene Oxide Dimer Acid (HFPO-DA or GenX). *Environ Health Perspect, 128*, 27006.

Buck, R. C., Franklin, J., Berger, U., Conder, J. M., Cousins, I. T., de Voogt, P., Jensen, A. A., Kannan, K., Mabury, S. A., van Leeuwen, S. P., 2011. Perfluoroalkyl and polyfluoroalkyl substances in the environment: terminology, classification, and origins. *Integr Environ Assess Manag, 7*, 513-541.

Conley, J. M., Lambright, C. S., Evans, N., Strynar, M. J., McCord, J., McIntyre, B. S., Travlos, G. S., Cardon, M. C., Medlock-Kakaley, E., Hartig, P. C., Wilson, V. S., Jr. L. E. G., 2019. Adverse maternal, fetal, and postnatal effects of hexafluoropropylene oxide dimer acid (GenX) from oral gestational exposure in Sprague-Dawley rats. *Environ Health Persp, 127*, 37008.

Cui, R. N., Li, C. Y., Wang, J. S., Dai, J. Y., 2019. Induction of hepatic miR-34a by perfluorooctanoic acid regulates metabolism-related genes in mice. *Environ Pollut, 244*, 270-278.

Dan A. Liebermann, B. H., 2013. Gadd45 stress sensor genes.Springer,New York.

Dewitt, J. C., 2015. Toxicological Effects of Perfluoroalkyl and Polyfluoroalkyl Substances.Humana press,New York.

ECHA, 2019. European Chemicals Agency. Candidate list of substances of very high concern for authorisation. https://echa.europa.eu/candidate-list-table.

Fromme, H., Wockner, M., Roscher, E., Volkel, W., 2017. ADONA and perfluoroalkylated substances in plasma samples of German blood donors living in South Germany. *Int J Hyg Envir Heal, 220*, 455-460.

Gebbink, W. A., Asseldonk, L. V., Leeuwen, S. P. J. V., 2017. Presence of Emerging Per- and Polyfluoroalkyl Substances (PFASs) in River and Drinking Water near a Fluorochemical Production Plant in the Netherlands. *Environ Sci Technol, 51*, 11057-11065.

Gordon, S. C., 2011. Toxicological evaluation of ammonium 4,8-dioxa-3H-perfluorononanoate, a new emulsifier to replace ammonium perfluorooctanoate in fluoropolymer manufacturing. *Regul Toxicol Pharm, 59*, 64-80.

Guo, H., Wang, J. H., Yao, J. Z., Sun, S. J., Sheng, N., Zhang, X. W., Guo, X. J., Guo, Y., Sun, Y., Dai, J. Y., 2019. Comparative Hepatotoxicity of Novel PFOA Alternatives (Perfluoropolyether Carboxylic Acids) on Male Mice. *Environ Sci Technol, 53*, 3929-3937.

Hogue, C., 2019. The hunt is on for GenX chemicals in people : Analysis of North Carolina residents' blood for Chemours PFAS yields surprises. *Chemical and Engineering News, 97*.

Hopkins, Z. R., Sun, M., DeWitt, J. C., Knappe, D. R. U., 2018. Recently Detected Drinking Water Contaminants: GenX and Other Per- and Polyfluoroalkyl Ether Acids. *J Am Water Works Ass, 110*, 13-28.

Kaiser, A. M., Attardi, L. D., 2018. Deconstructing networks of p53-mediated tumor suppression in vivo. *Cell Death Differ, 25*, 93-103.

Kharitonenkov, A., Shiyanova, T. L., Koester, A., Ford, A. M., Micanovic, R., Galbreath, E. J., Sandusky, G. E., Hammond, L. J., Moyers, J. S., Owens, R. A., Gromada, J., Brozinick, J. T., Hawkins, E. D., Wroblewski, V. J., Li, D. S., Mehrbod, F., Jaskunas, S. R., Shanafelt, A. B., 2005. FGF-21 as a novel metabolic regulator. *J Clin Invest, 115*, 1627-1635.

Kotlarz, N., McCord, J., Collier, D., Lea, C. S., Strynar, M., Lindstrom, A. B., Wilkie, A. A., Islam, J. Y., Matney, K., Tarte, P., Polera, M. E., Burdette, K., DeWitt, J., May, K., Smart, R. C., Knappe, D. R. U., Hoppin, J. A., 2020. Measurement of novel, drinking water-associated PFAS in blood from adults and children in Wilmington, North Carolina. *Environ Health Persp, 128*, 77005.

Lau, C., Anitole, K., Hodes, C., Lai, D., Pfahles-Hutchens, A., Seed, J., 2007. Perfluoroalkyl acids: a review of monitoring and toxicological findings. *Toxicol Sci, 99*, 366-394.

Levada, K., Guldiken, N., Zhang, X. J., Vella, G., Mo, F. R., James, L. P., Haybaeck, J., Kessler, S. M., Kiemer, A. K., Ott, T., Hartmann, D., Huser, N., Ziol, M., Trautwein, C., Strnad, P., 2018. Hsp72 protects against liver injury via attenuation of hepatocellular death, oxidative stress, and JNK signaling. *J Hepatol, 68*, 996-1005.

Luo, Y., McKeehan, W. L., 2013. Stressed Liver and Muscle Call on Adipocytes with FGF21. *Front Endocrinol (Lausanne), 4*, 194.

Mak, Y. L., Taniyasu, S., Yeung, L. W. Y., Lu, G. H., Jin, L., Yang, Y. L., Lam, P. K. S., Kannan, K., Yamashita, N., 2009. Perfluorinated Compounds in Tap Water from China and Several Other Countries. *Environ Sci Technol, 43*, 4824-4829.

Nakade, K., Lin, C. S., Chen, X. Y., Tsai, M. H., Wuputra, K., Zhu, Z. W., Pan, J. Z., Yokoyama, K. K., 2017. Jun dimerization protein 2 controls hypoxia-induced replicative senescence via both the p16(Ink4a)-pRb and Arf-p53 pathways. *FEBS Open Bio, 7*, 1793-1804.

Ohmori, K., Kudo, N., Katayama, K., Kawashima, Y., 2003. Comparison of the toxicokinetics between perfluorocarboxylic acids with different carbon chain length. *Toxicology, 184*, 135-140.

Ohta, H., Itoh, N., 2014. Roles of FGFs as adipokines in adipose tissue development, remodeling, and metabolism. *Front Endocrinol, 5*, 18.

Pilkis, S. J., Claus, T. H., Kurland, I. J., Lange, A. J., 1995. 6-Phosphofructo-2-Kinase/Fructose-2,6-Bisphosphatase - a Metabolic Signaling Enzyme. *Annu Rev Biochem, 64*, 799-835.

Ramji, D. P., Foka, P.,2002. CCAAT/enhancer-binding proteins: structure, function and regulation. *Biochem J, 365*, 561-575.

Sakakibara, R., Kato, M., Okamura, N., Nakagawa, T., Komada, Y., Tominaga, N., Shimojo, M., Fukasawa, M., 1997. Characterization of a human placental fructose-6-phosphate 2-kinase fructose-2,6-bisphosphatase. *J Biochem-Tokyo, 122*, 122-128.

Secretariat of the Basel, Rotterdam and Stockholm Conventions, 2019. POPRC recommendations for listing chemicals – chemicals reviewed. http://chm.pops.int/Convention/POPsReviewCommittee/Chemicals/tabid/243/Default.aspx.

Sheng, N., Pan, Y. T., Guo, Y., Sun, Y., Dai, J. Y., 2018. Hepatotoxic Effects of Hexafluoropropylene Oxide Trimer Acid (HFPO-TA), A Novel Perfluorooctanoic Acid (PFOA) Alternative, on Mice. *Environ Sci Technol, 52*, 8005-8015.

Shi, L., Pan, H., Liu, Z., Xie, J., Han, W., 2017. Roles of PFKFB3 in cancer. *Signal Transduct Target Ther, 2*, 17044.

Strynar, M., Dagnino, S., McMahen, R., Liang, S., Lindstrom, A., Andersen, E., McMillan, L., Thurman, M., Ferrer, I., Ball, C., 2015. Identification of Novel Perfluoroalkyl Ether Carboxylic Acids (PFECAs) and Sulfonic Acids (PFESAs) in Natural Waters Using Accurate Mass Time-of-Flight Mass Spectrometry (TOFMS). *Environ Sci Technol, 49*, 11622-11630.

Sun, M., Arevalo, E., Strynar, M., Lindstrom, A., Richardson, M., Kearns, B., Pickett, A., Smith, C., Knappe, D. R. U., 2016. Legacy and Emerging Perfluoroalkyl Substances Are Important Drinking Water Contaminants in the Cape Fear River Watershed of North Carolina. *Environ Sci Tech Let, 3*, 415-419.

Sun, S. J., Guo, H., Wang, J. S., Dai, J. Y., 2019. Hepatotoxicity of perfluorooctanoic acid and two emerging alternatives based on a 3D spheroid model. *Environ Pollut, 246*, 955-962.

Tomasini, R., Samir, A. A., Pebusque, M. J., Calvo, E. L., Totaro, S., Dagorn, J. C., Dusetti, N. J., Iovanna, J. L., 2002. P53-dependent expression of the stress-induced protein (SIP). *Eur J Cell Biol, 81*, 294-301.

Tonnelier, A., Coecke, S., Zaldivar, J. M., 2012. Screening of chemicals for human bioaccumulative potential with a physiologically based toxicokinetic model. *Arch Toxicol, 86*, 393-403.

Vanden Heuvel, J., Thompson, J., Frame, S., Gillies, P., 2006. Differential activation of nuclear receptors by perfluorinated fatty acid analogs and natural fatty acids: a comparison of human, mouse, and rat peroxisome proliferator-activated receptor-alpha, -beta, and -gamma, liver X receptor-beta, and retinoid X receptor-alpha. *Toxicol Sci, 92*, 476-489.

Wang, J., Wang, X., Sheng, N., Zhou, X., Cui, R., Zhang, H., Dai, J., 2017. RNA-sequencing analysis reveals the hepatotoxic mechanism of perfluoroalkyl alternatives, HFPO2 and HFPO4, following exposure in mice. *J Appl Toxicol, 37*, 436-444.

Wang, J. X., Shi, G. H., Yao, J. Z., Sheng, N., Cui, R. N., Su, Z. B., Guo, Y., Dai, J. Y., 2020. Perfluoropolyether carboxylic acids (novel alternatives to PFOA) impair zebrafish posterior swim bladder development via thyroid hormone disruption. *Environ Int, 134*.

Wang, Z. Y., Cousins, I. T., Scheringer, M., Hungerbuhler, K., 2013. Fluorinated alternatives to long-chain perfluoroalkyl carboxylic acids (PFCAs), perfluoroalkane sulfonic acids (PFSAs) and their potential precursors. *Environ Int, 60*, 242-248.

Wang, Z. Y., DeWitt, J., Higgins, C. P., Cousins, I. T.,2018. A Never-Ending Story of Per- and Polyfluoroalkyl Substances (PFASs)? *Environ Sci Technol, 52*, 3325-3325.

Weber, G., 1977. Enzymology of Cancer-Cells. *New Engl J Med, 296*, 486-493.

Xiao, F., 2017. Emerging poly- and perfluoroalkyl substances in the aquatic environment: A review of current literature. *Water Res, 124*, 482-495.

Yao, J., Pan, Y., Sheng, N., Su, Z., Guo, Y., Wang, J., Dai, J., 2020. Novel Perfluoroalkyl Ether Carboxylic Acids (PFECAs) and Sulfonic Acids (PFESAs): Occurrence and Association with Serum Biochemical Parameters in Residents Living Near a Fluorochemical Plant in China. *Environmental Science Technology, 54*, 13389-13398.

Zhang, C. H., Hopkins, Z. R., McCord, J., Strynar, M. J., Knappe, D. R. U., 2019. Fate of Per- and Polyfluoroalkyl Ether Acids in the Total Oxidizable Precursor Assay and Implications for the Analysis of Impacted Water. *Environ Sci Tech Let, 6*, 662-668.

Zhang, H. X., Zhou, X. J., Sheng, N., Cui, R. N., Cui, Q. Q., Guo, H., Guo, Y., Sun, Y., Dai, J. Y., 2018. Subchronic Hepatotoxicity Effects of 6:2 Chlorinated Polyfluorinated Ether Sulfonate (6:2 Cl-PFESA), a Novel Perfluorooctanesulfonate (PFOS) Alternative, on Adult Male Mice. *Environ Sci Technol, 52*, 12809-12818.

## Figure Legends

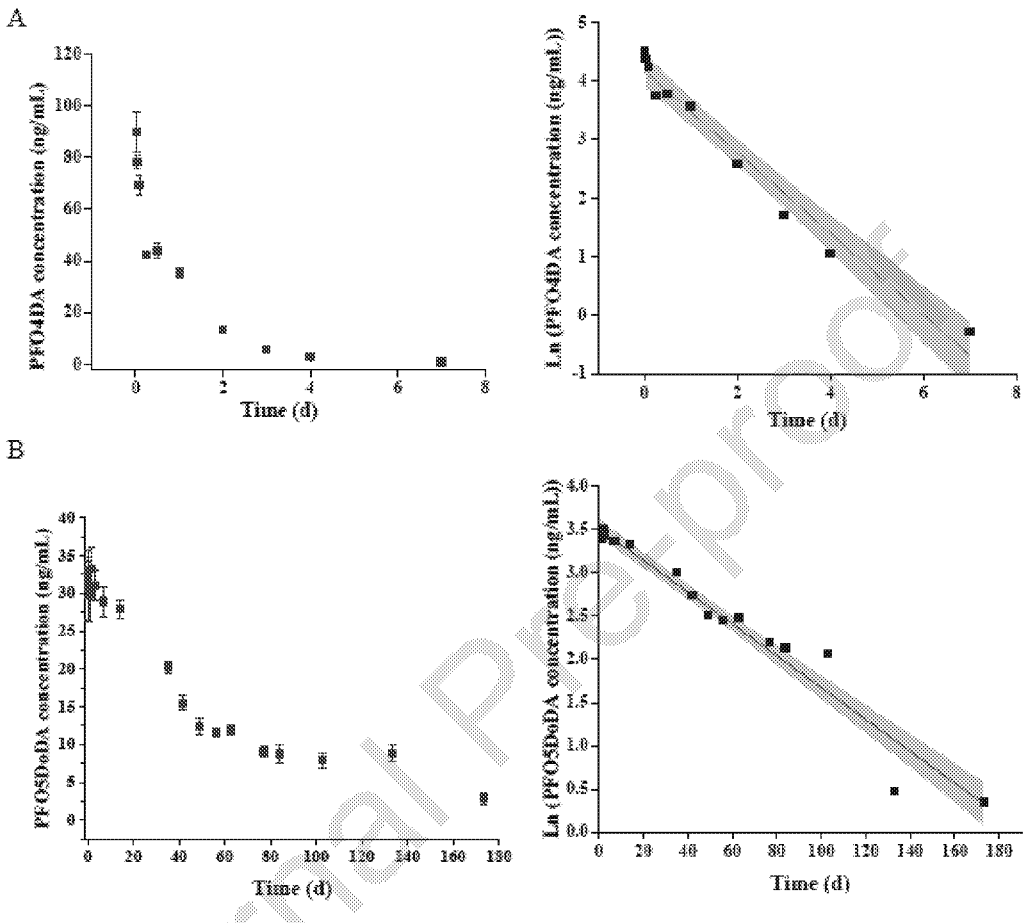


**Fig. 1** Serum concentration-time curve of PFO4DA and PFO5DoDA (n = 4). Changes in serum chemical concentration with time following a single intravenous injection of 10 μg/kg PFO4DA (left panel) and concentration-time curve plotted semi-logarithmically (right panel) (A). Changes in serum chemical concentration with time following a single intravenous injection of 10 μg/kg PFO5DoDA (left panel) and concentration-time curve plotted semi-logarithmically (right panel) (B).

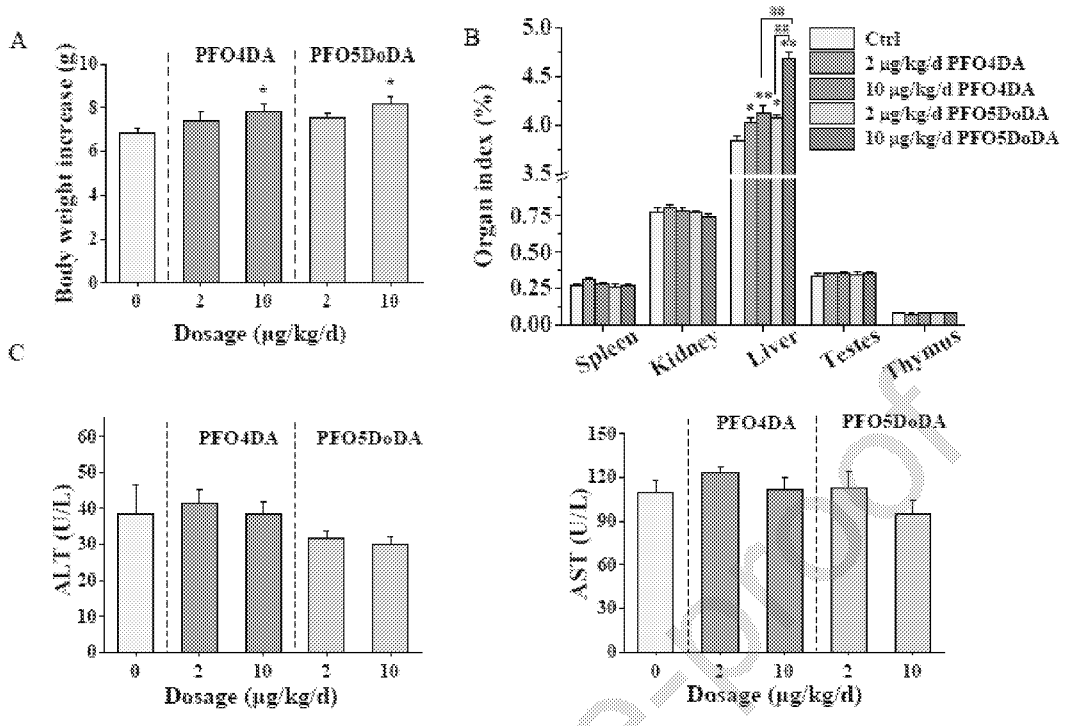


**Fig. 2** Characteristics of mice after 140 d of PFO4DA or PFO5DoDA treatment. Changes in body weight (A) and relative organ weight (B); Serum indicators for liver damage, alanine transaminase (ALT) and aspartate transaminase (AST) (C). Data are means ± SE (n = 6). Differences were evaluated with one-way analysis of variance (ANOVA) followed by Duncan's multiple range test, and $p < 0.05$ between groups was considered statistically significant. * control vs. treatment $p < 0.05$; # groups linking with line $p < 0.05$; double symbols mean $p < 0.01$.

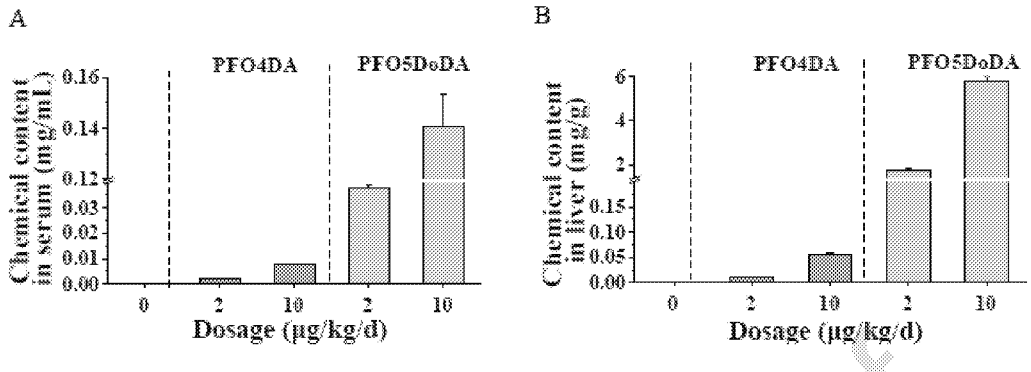


**Fig. 3** PFO4DA and PFO5DoDA content in serum (A) and liver (B) after 140 d of exposure.

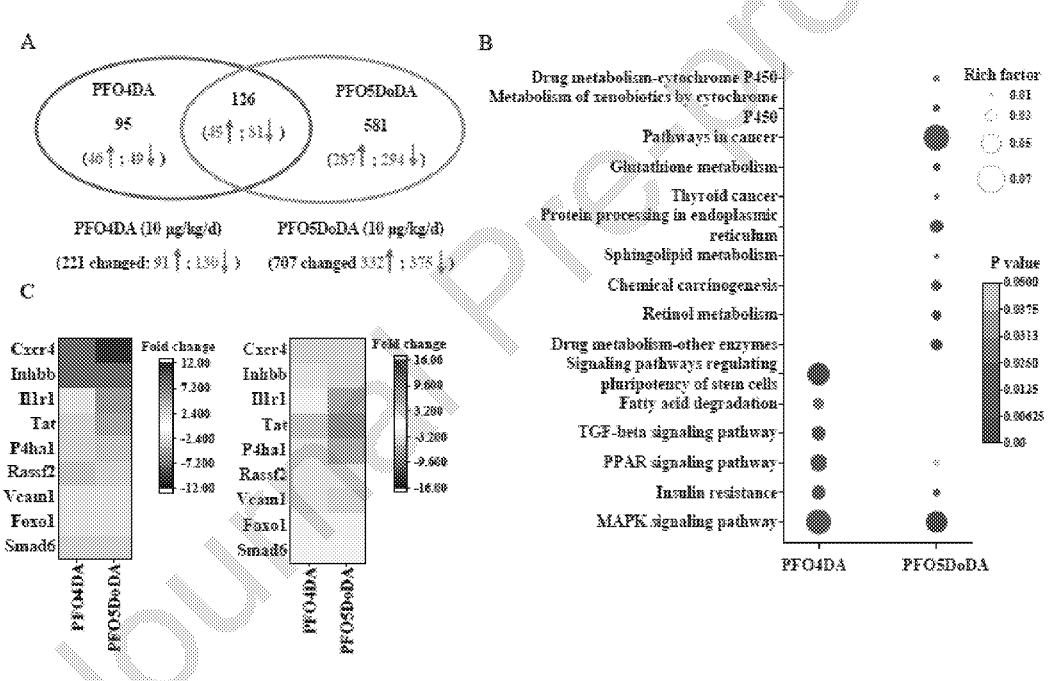


**Fig. 4** Hepatic mRNA transcriptome in 10 μg/kg/d of PFO4DA and PFO5DoDA groups. Venn graph of DEGs after treatment (A). KEGG enrichment of DEGs (B). Heatmap of DEGs by RNA-seq (left panel) and qRT-PCR verification (right panel) (C).

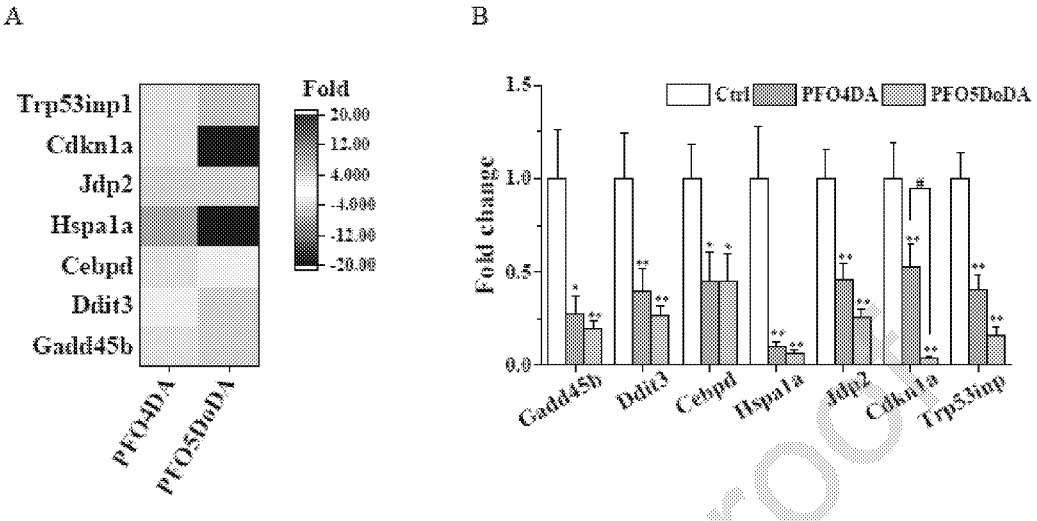


**Fig. 5** Suppression of stress-sensing genes by PFO4DA/PFO5DoDA treatment. Heatmap of DEGs involved in stress based on RNA-seq after 140 d of 10 μg/kg/d PFO4DA and PFO5DoDA treatment (A); qRT-PCR verification of DEGs involved in stress sensing after 140 d of 10 μg/kg/d PFO4DA and PFO5DoDA treatment (B). Data are means ± SE (n = 3 for RNA-seq and n = 6 for PCR assay). Differences were evaluated by one-way analysis of variance (ANOVA) followed by Duncan's multiple range test, and $p < 0.05$ between groups was considered statistically significant. * control vs. treatment $p < 0.05$; # PFO4DA vs. PFO5DoDA $p < 0.05$; double symbols mean $p < 0.01$.

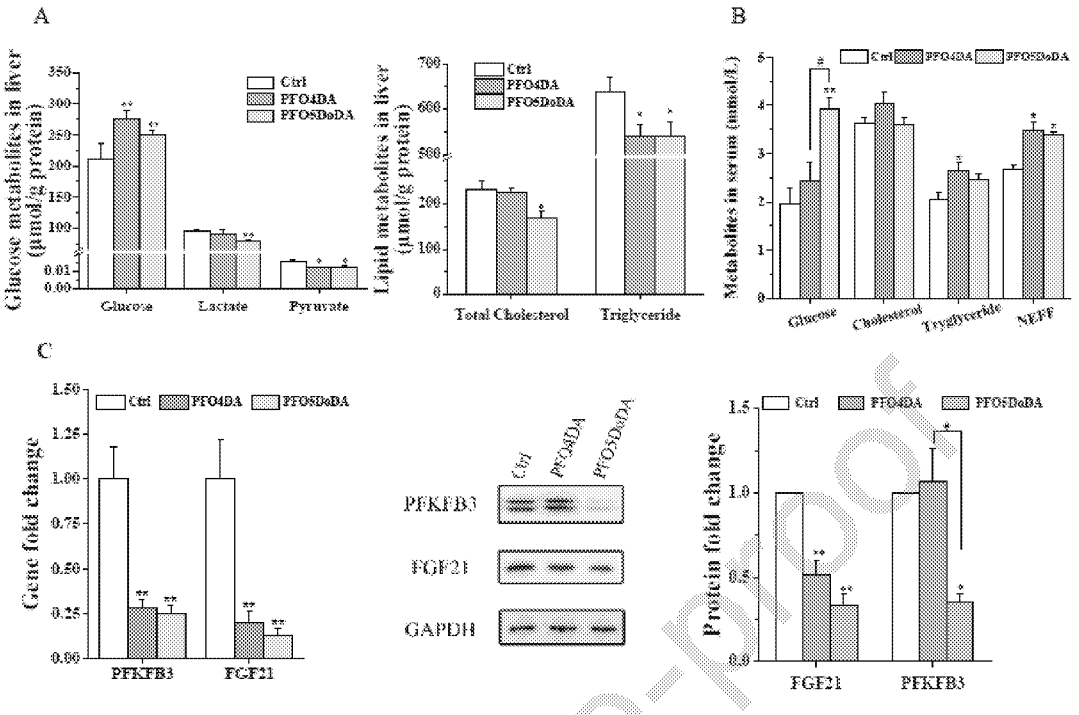


**Fig. 6** Metabolites after 140 d of PFO4DA and PFO5DoDA treatment. Metabolites, including glucose, pyruvate lactate, cholesterol, and triglycerides in liver (A); Glucose, cholesterol, triglycerides, and NEFF in serum (B); mRNA and protein levels of *Pfkfb3* and *Fgf21* (C). Data are means ± SE (n = 6). Differences were evaluated by one-way analysis of variance (ANOVA) followed by Duncan's multiple range test, and $p < 0.05$ between groups was considered statistically significant. * control vs. treatment $p < 0.05$; # PFO4DA vs. PFO5DoDA $p < 0.05$; double symbols mean $p < 0.01$.

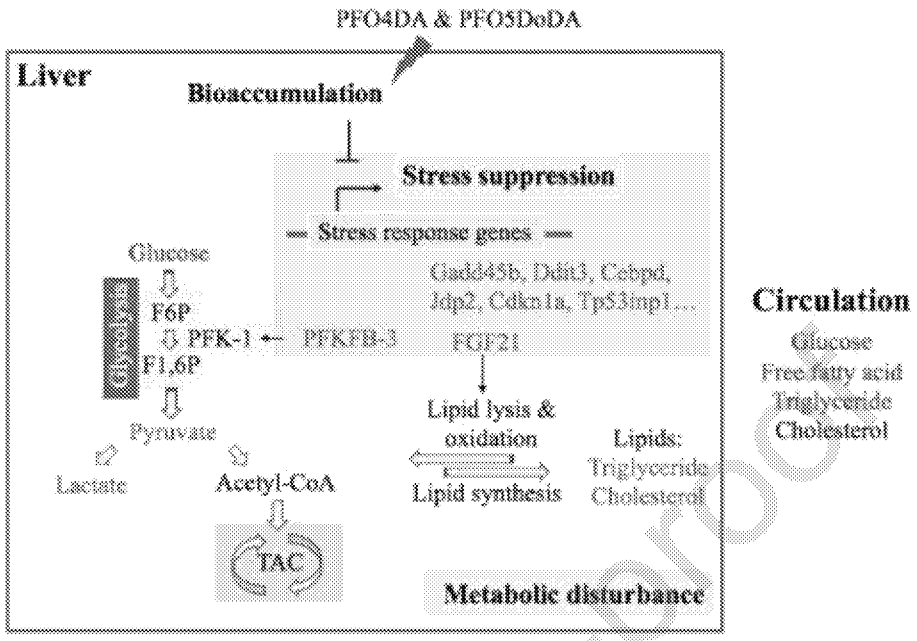


**Fig. 7** Proposed effects of chronic PFO4DA and PFO5DoDA exposure on liver.

# Credit author statement

Investigation: Jiamiao Chen, Hongyuan Li, Jingzhi Yao and Hongxia Zhang.

Formal analysis: Hua Guo.

Funding acquisition; Jianshe Wang and Nan Sheng.

Project administration: Jianshe Wang, Yong Guo and Jiayin Dai.

Writing-Review & Editing: Jianshe Wang.

**Declaration of interests**

☒ The authors declare that they have no known competing financial interests or personal relationships

that could have appeared to influence the work reported in this paper.

☐The authors declare the following financial interests/personal relationships which may be considered

as potential competing interests:

Graphic abstract

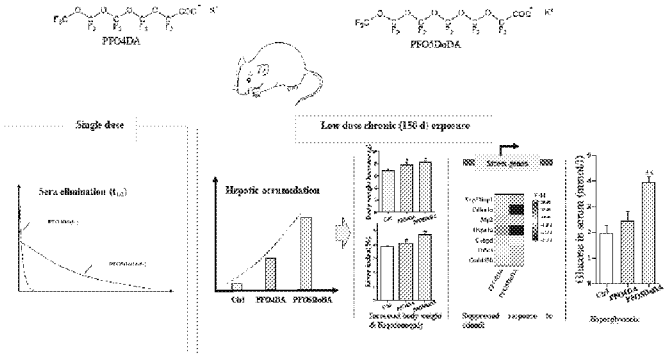

## Highlights

Increased $-OCF_2$ in PFO5DoDA greatly slowed its serum elimination rate compared with PFO4DA.

Long-term low-dose intake of PFO4DA and PFO5DoDA increased body weight in male mice.

PFO4DA and PFO5DoDA suppressed a wide array of stimulus sensing and response signals.

PFO4DA and PFO5DoDA reduced hepatic glycolysis but increased serum glucose and lipid levels.

PFO5DoDA showed similar but stronger bioaccumulation and toxicity in the liver than PFO4DA.